



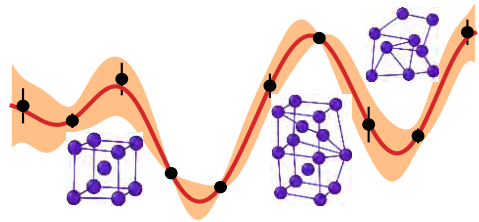
EUROfusion



**Finnfusion Annual Seminar  
2024**



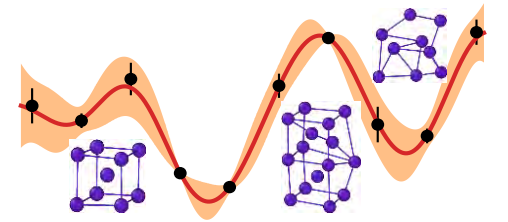
# Radiation Damage Simulations in W-based Alloys



**Guanying Wei**

**Jesper Byggmästar, Kai Nordlund, Flyura Djurabekova**

*University of Helsinki, Accelerator Laboratory*





# Outline

- Background
- The critical role of vanadium in radiation damage of W-based alloys
- Ongoing work
- Summary



# *Background*



# W for fusion reactors

Tungsten (W) is an important candidate for plasma-facing materials.

## Advantages:

- high melting point
- good thermal conductivity
- high sputtering resistance

## Disadvantages:

- ❑ brittleness and low ductility at room temperature
- ❑ high ductile-brittle transition temperature (DBTT)
- ❑ radiation hardening and embrittlement

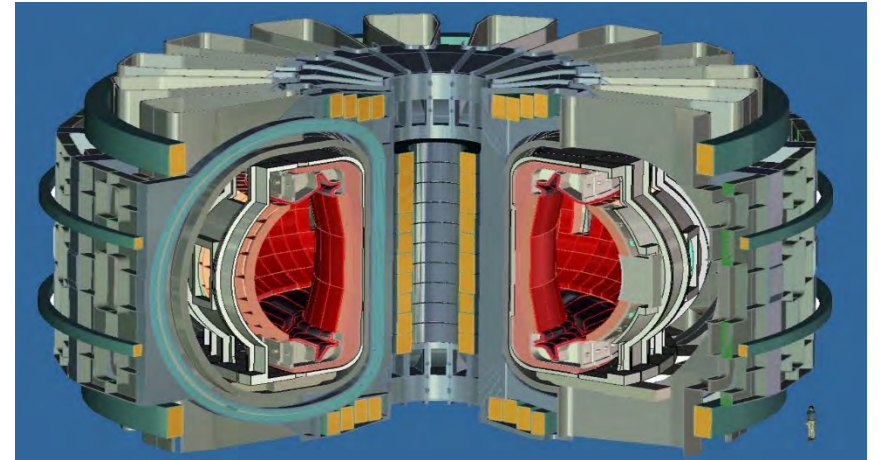
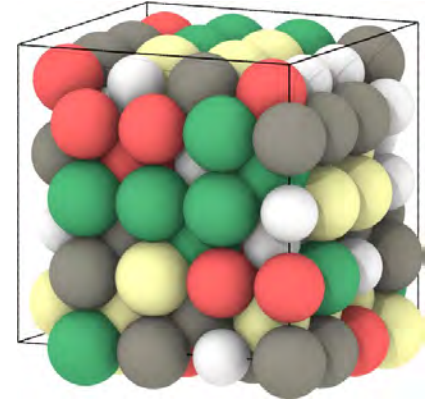


Illustration of a tokamak reactor (from iter.org)



# W-based alloys for fusion reactors

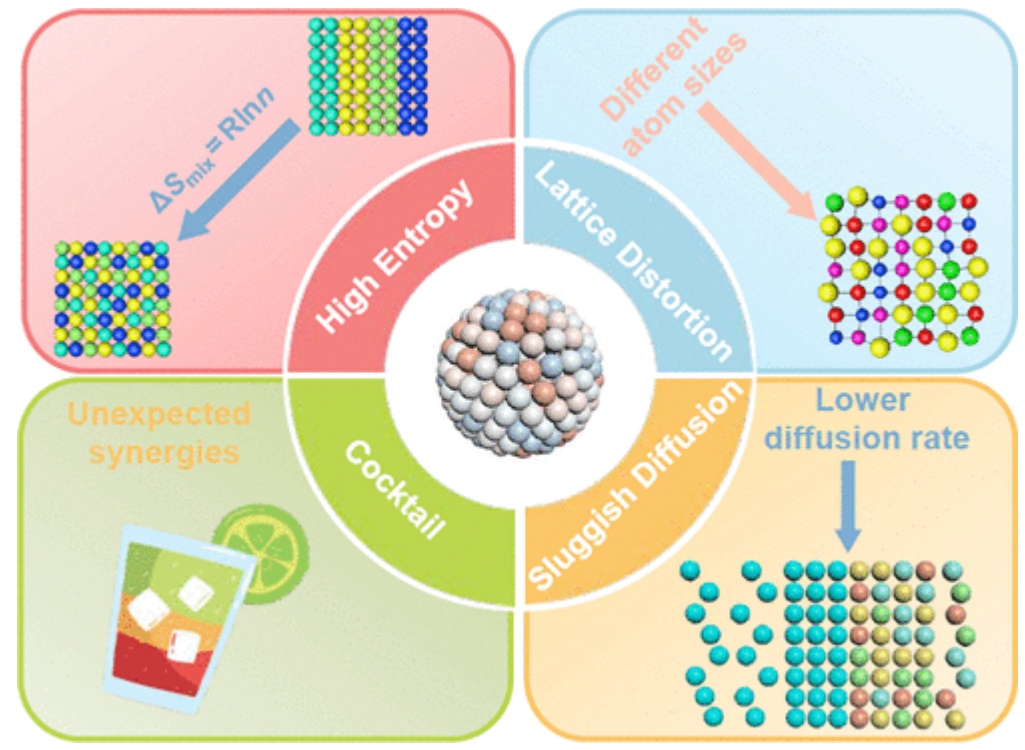


High-entropy alloy

Periodic Table of the Elements

Uertex42  
Free Downloads at Uertex2.com

GROUP 1 IA	Common Constants																18 VIIIA								
1 H Hydrogen	2 He Helium																	3 Li Lithium	4 Be Beryllium	5 B Boron	6 C Carbon	7 N Nitrogen	8 O Oxygen	9 F Fluorine	10 Ne Neon
2 3 4 5 6 7 8 9 10 11 12 13 14 15 16 17 18	19 K Potassium	20 Ca Calcium	21 Sc Scandium	22 Ti Titanium	23 V Vanadium	24 Cr Chromium	25 Mn Manganese	26 Fe Iron	27 Co Cobalt	28 Ni Nickel	29 Cu Copper	30 Zn Zinc	31 Ga Gallium	32 Ge Germanium	33 As Arsenic	34 Se Selenium	35 Br Bromine	36 Kr Krypton							
3 4 5 6 7 8 9 10 11 12 13 14 15 16 17 18	37 Rb Rubidium	38 Sr Strontium	39 Y Yttrium	40 Zr Zirconium	41 Nb Niobium	42 Mo Molybdenum	43 Tc Technetium	44 Ru Ruthenium	45 Rh Rhodium	46 Pd Palladium	47 Ag Silver	48 Cd Cadmium	49 In Indium	50 Sn Tin	51 Sb Antimony	52 Te Tellurium	53 I Iodine	54 Xe Xenon							
6 7 8 9 10 11 12 13 14 15 16 17 18	55 Cs Cesium	56 Ba Barium	Lanthanide Series																81 Tl Thallium	82 Pb Lead	83 Bi Bismuth	84 Po Polonium	85 At Astatine	86 Rn Radon	
7 8 9 10 11 12 13 14 15 16 17 18	87 Fr Francium	88 Ra Radium	Actinide Series																113 Nh Nihonium	114 Fl Flerovium	115 Mc Moscovium	116 Lv Livermorium	117 Ts Tennessine	118 Og Oganesson	



Adding alloying elements for solid solution strengthening



*The critical role of vanadium in radiation damage  
of W-based alloys*

Wei, GY. Byggmästar, J. and Nordlund, K. and Djurabekova, F. et.al. Acta Materialia, 274,119991(2024).



# Element information

	Mo	Nb	Ta	V	W
Lattice constant (Å)	3.15	3.30	3.3058	3.03	3.180
Mass (u)	95.94	92.91	180.95	50.94	183.84
Melting point (°C)	2623	2477	3017	1910	3422

Tab.1: The lattice constant, mass, and melting point of the elements in the studied materials.



## Threshold displacement energy and primary damage

	W	WMo	WTa	WTaMo	WV	WTaV	WTaVMo	WTaVMoNb
$E_d$ (eV)	92.7±1.2	73.6±0.8	74.8±0.8	63.8±0.6	41.5±0.4	40.9±0.3	44.0±0.3	44.3±0.2
Number of FPs	7.4±0.5	6.4±0.6	11.3±0.7	9.5±0.5	19.8±1.1	23.1±1.1	18.3±0.8	18.1±0.9
$f_{\text{SIA}}$	0.56	0.38	0.39	0.35	0.27	0.19	0.17	0.16
$f_{\text{Vac}}$	0.16	0.24	0.38	0.31	0.64	0.70	0.59	0.56

Tab.2: **Average** threshold displacement energies  $E_d$  in considered materials were simulated at 300 K. The **average** number of FPs, fraction of interstitials in clusters  $f_{\text{SIA}}$  and fraction of vacancies in clusters  $f_{\text{Vac}}$  from 40 single cascades with 10 keV PKA energies in the considered materials. The error bar is the standard error of the average.



# MD simulation for overlapping cascades

## Materials:

W, WMo, WTa, WV, WTaMo, WTaV, WTaVMo, WTaVMoNb

## Box size :

354000 atoms

## Potential:

tabGAP (tabulated Gaussian approximation potentials)

## PKA energy:

10 keV

## Overlapping cascades:

One cascade + 10 ps relaxation + cascade + 10 ps relaxation + ...



# Defect accumulation

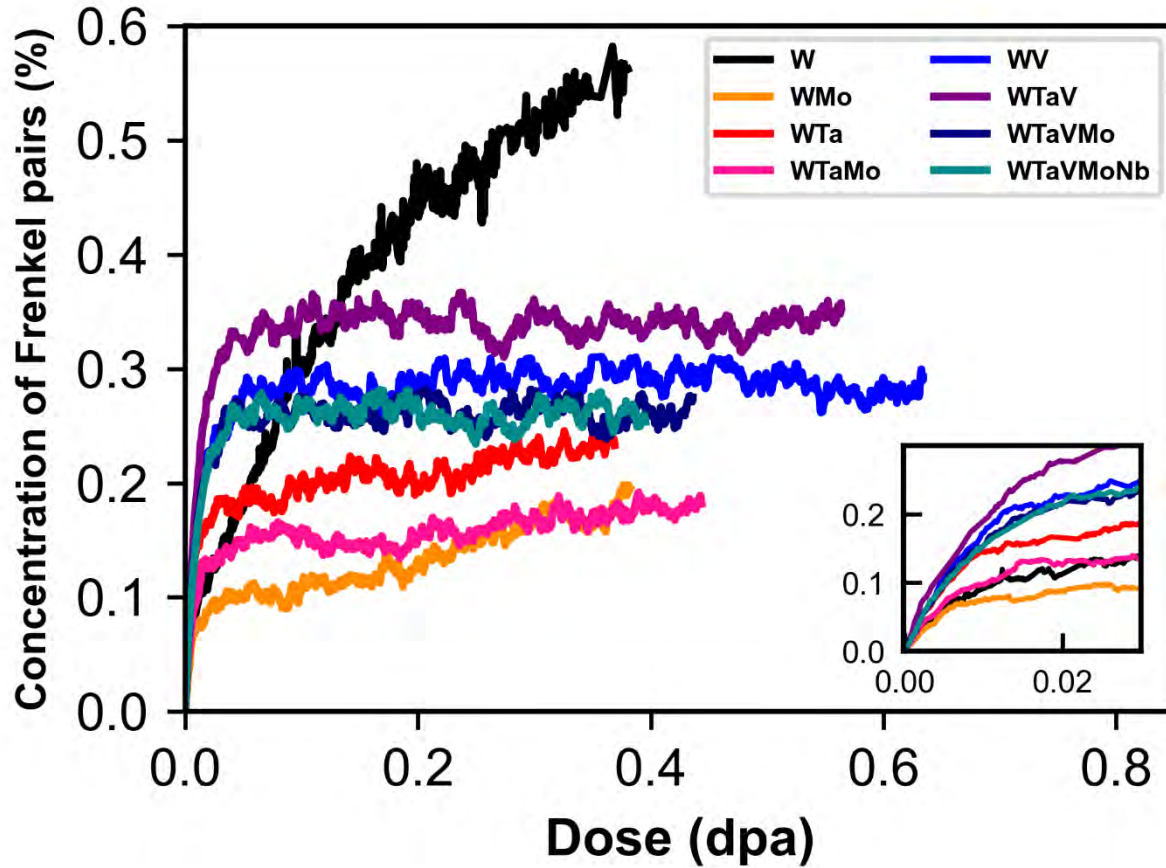


Fig.1: Defect concentration as a function of dose for considered materials. The inset is a zoom-in of the low-dose part, before saturation.



# Lattice swelling

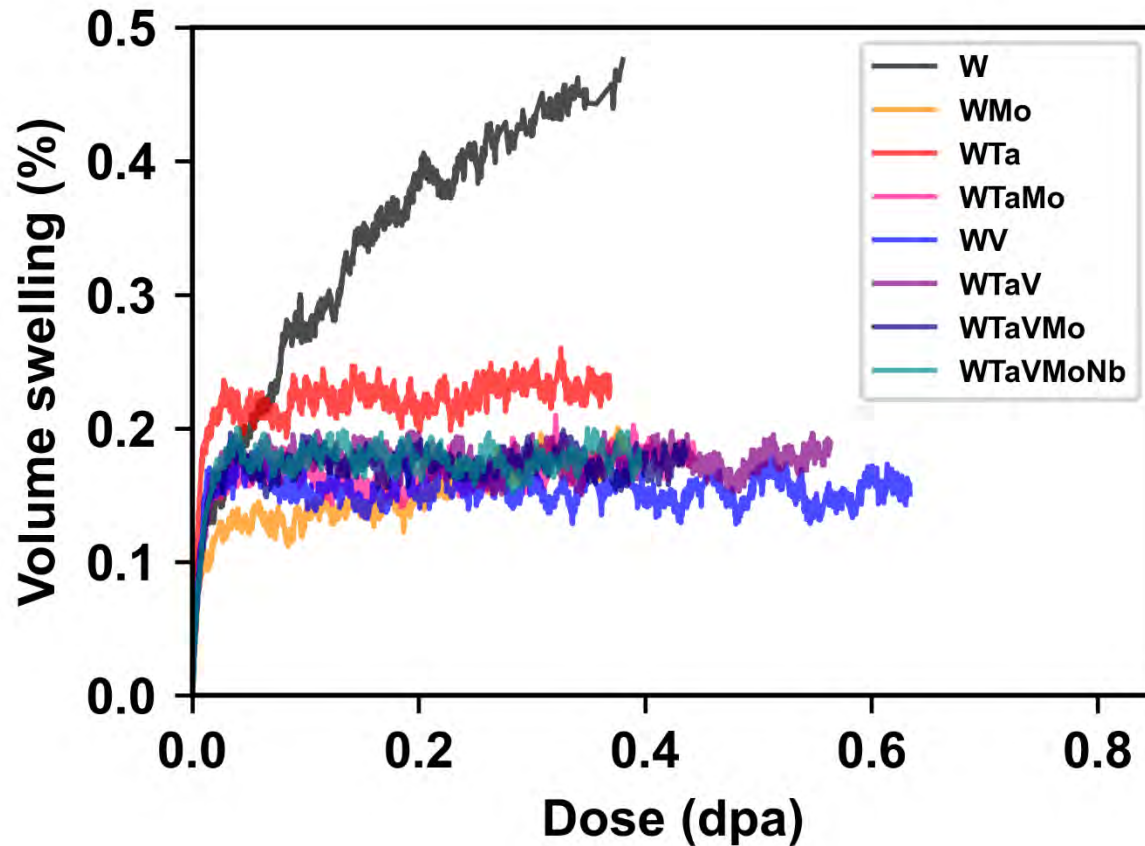
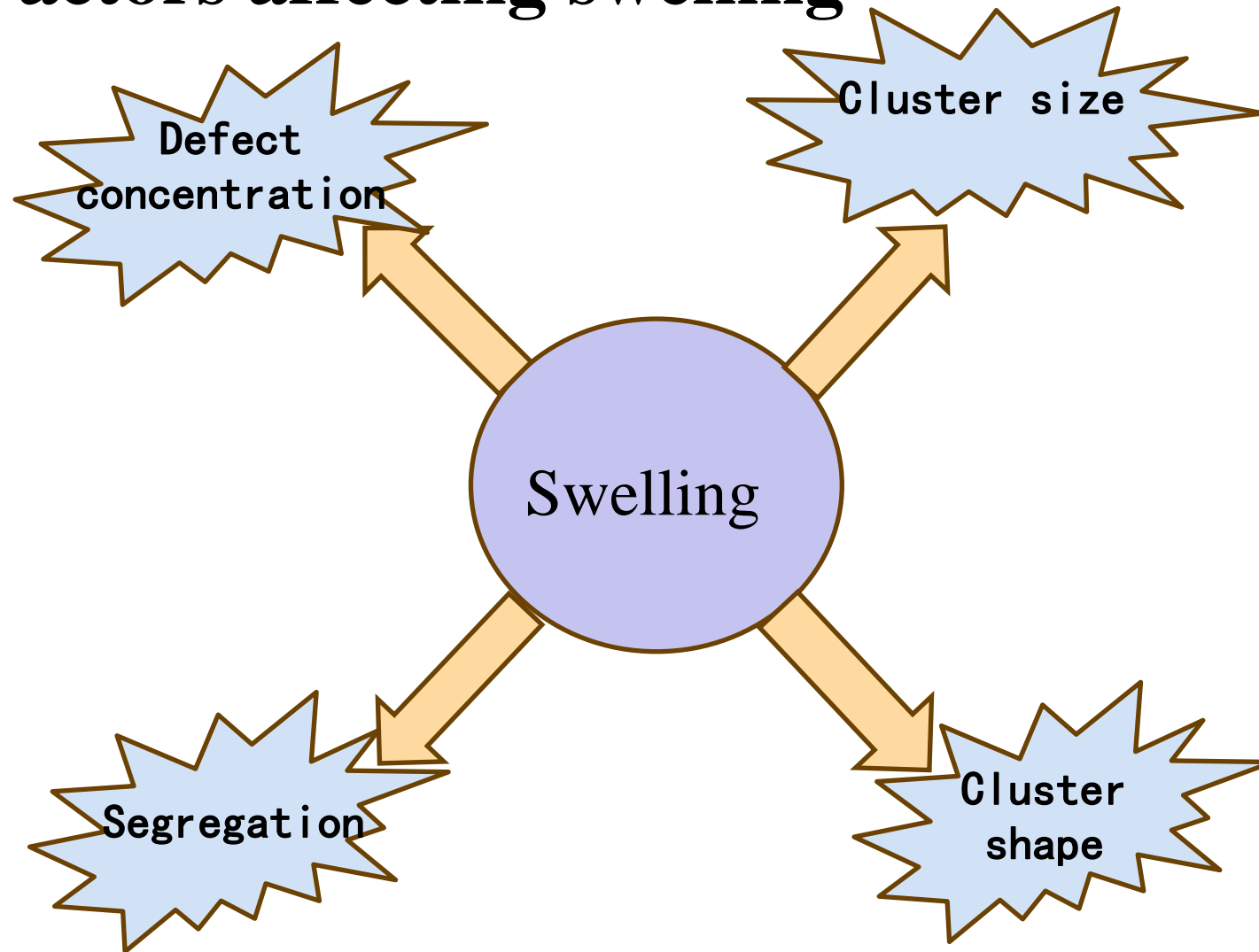


Fig.2: The volumetric swelling in all considered materials as a function of dose.



# Factors affecting swelling





# Defect clustering — cluster size

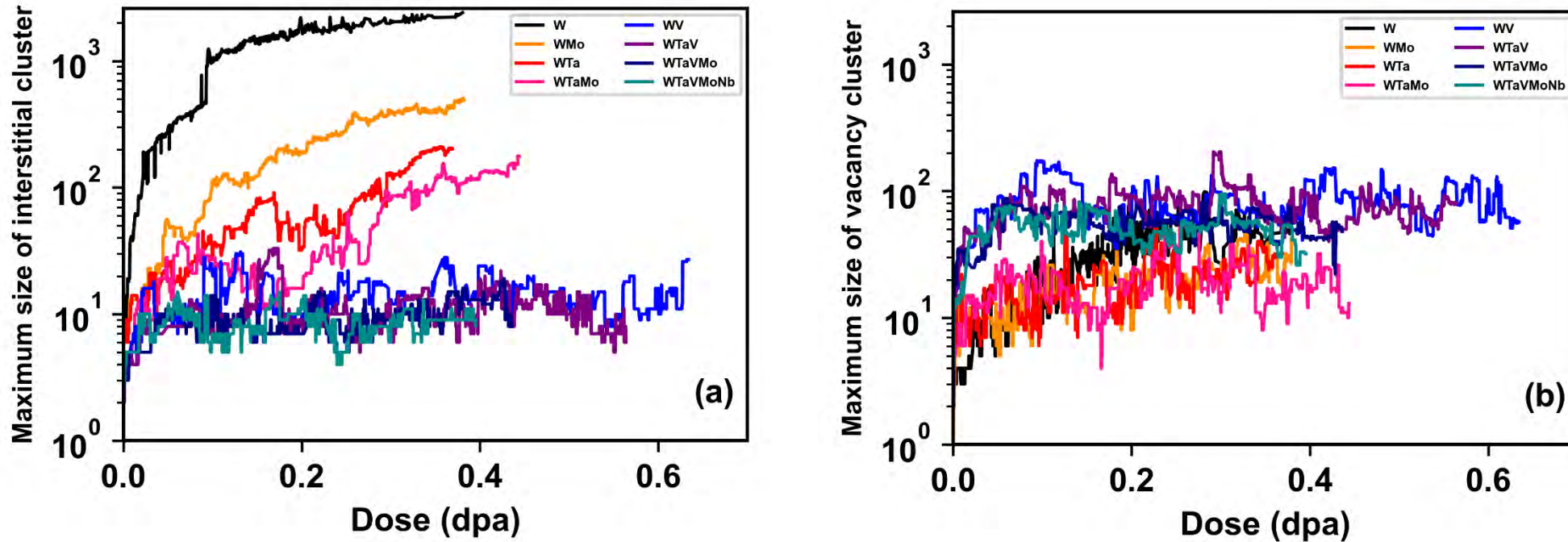


Fig.3: The maximum size as a function of dose for (a) interstitial clusters and (b) vacancy clusters in considered materials.



# Defect clustering — defect structures at around 0.3 dpa

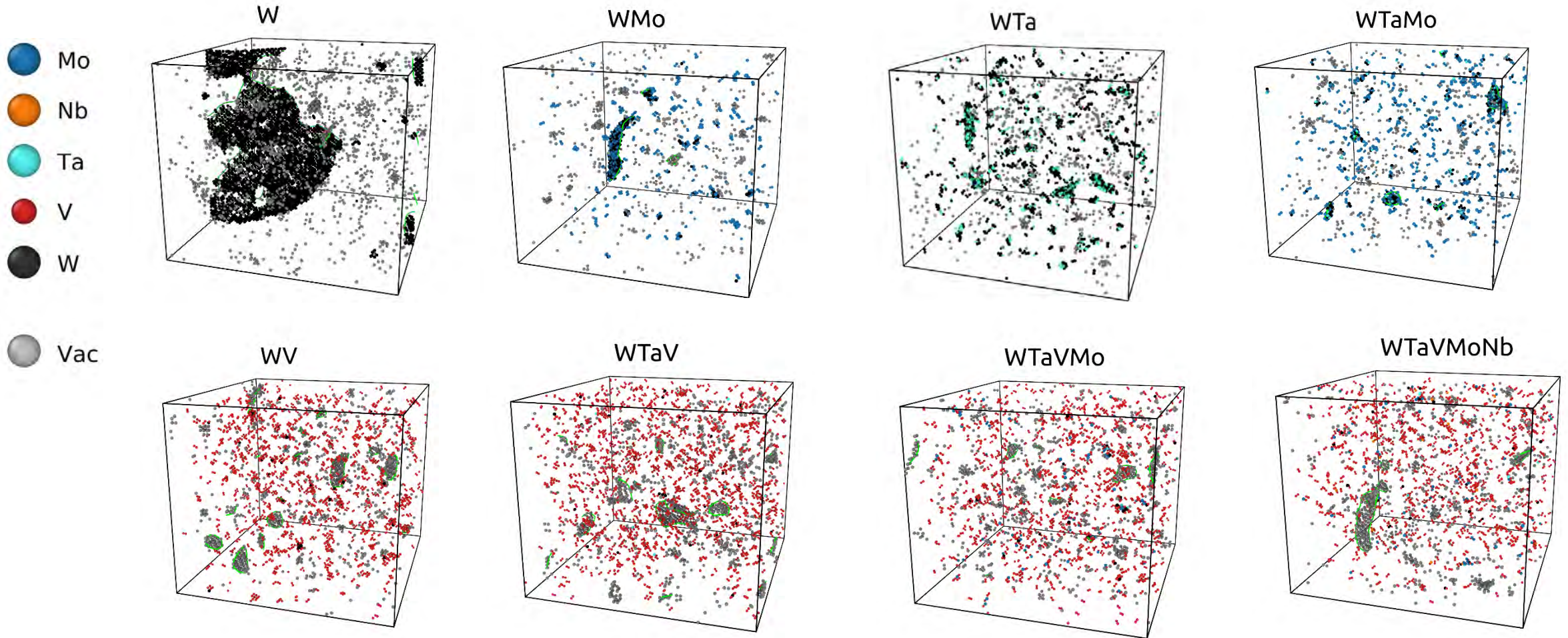


Fig.4: Snapshots of the defect structures in the considered materials at around 0.3 dpa. The atoms with different colours represent the different elements. The grey spheres represent vacancies. The green lines are  $1/2\langle 111 \rangle$  dislocation loops.



# Defect clustering — binding energy

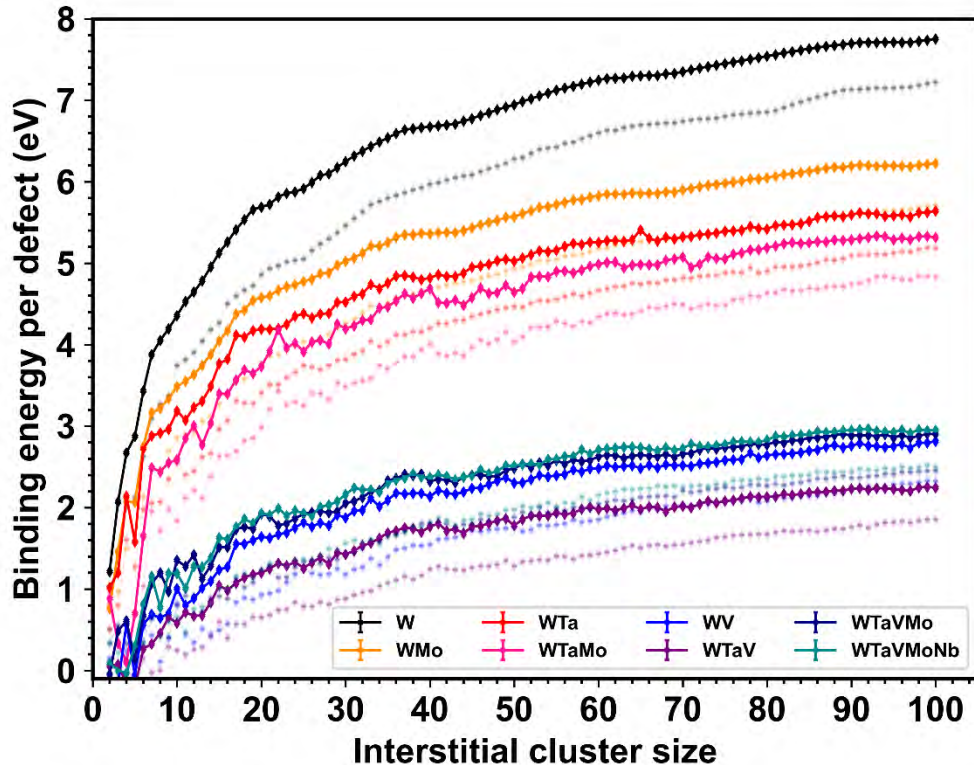


Fig.5: Binding energies per defect of  $1/2\langle 111 \rangle$  and  $\langle 100 \rangle$  interstitial loops. The solid line represents  $1/2\langle 111 \rangle$  loops and the semi-transparent line represents  $\langle 100 \rangle$  loops.

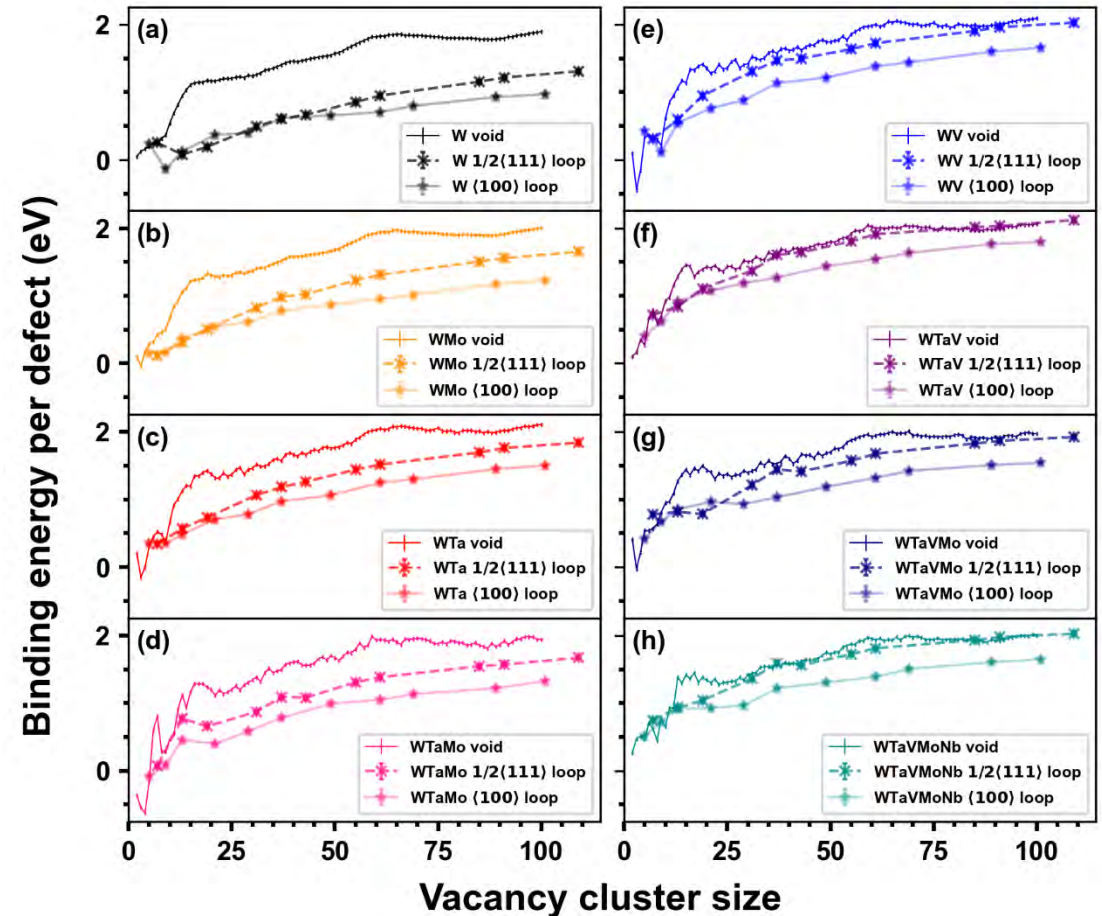


Fig.6: Binding energies per defect of  $1/2\langle 111 \rangle$  vacancy loops,  $\langle 100 \rangle$  vacancy loops and spherical voids for all considered materials.



# Defect clustering — migration energy

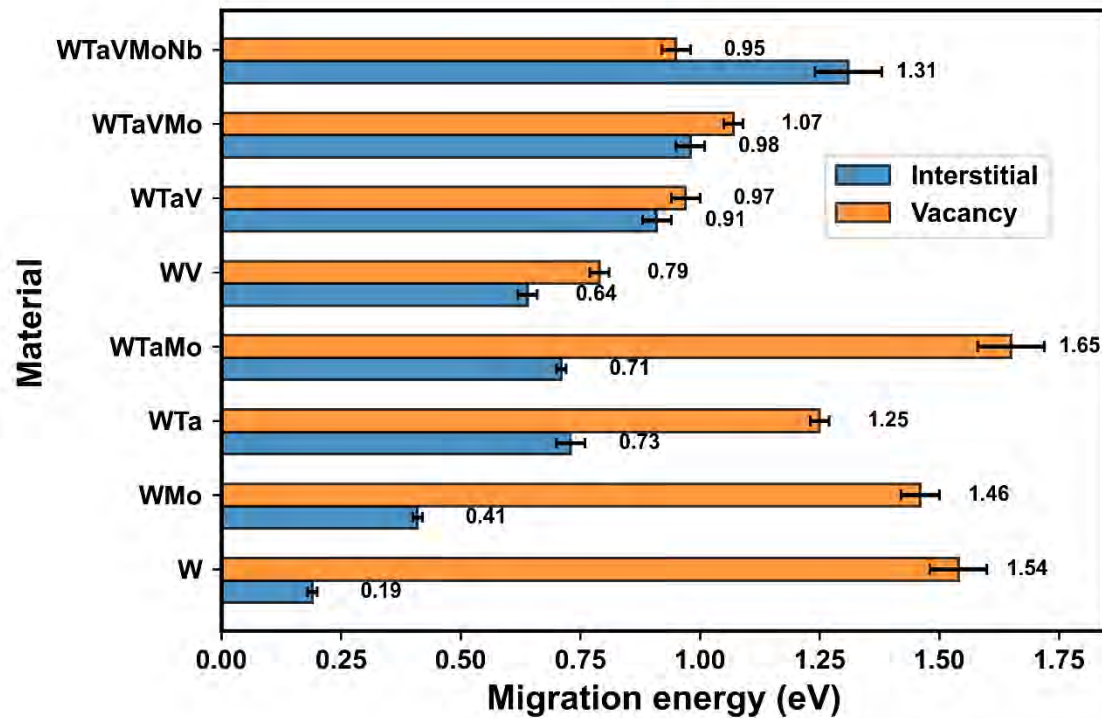


Fig.7: The interstitial and vacancy migration energy calculated by mean squared displacement (MSD) simulations for all considered materials.

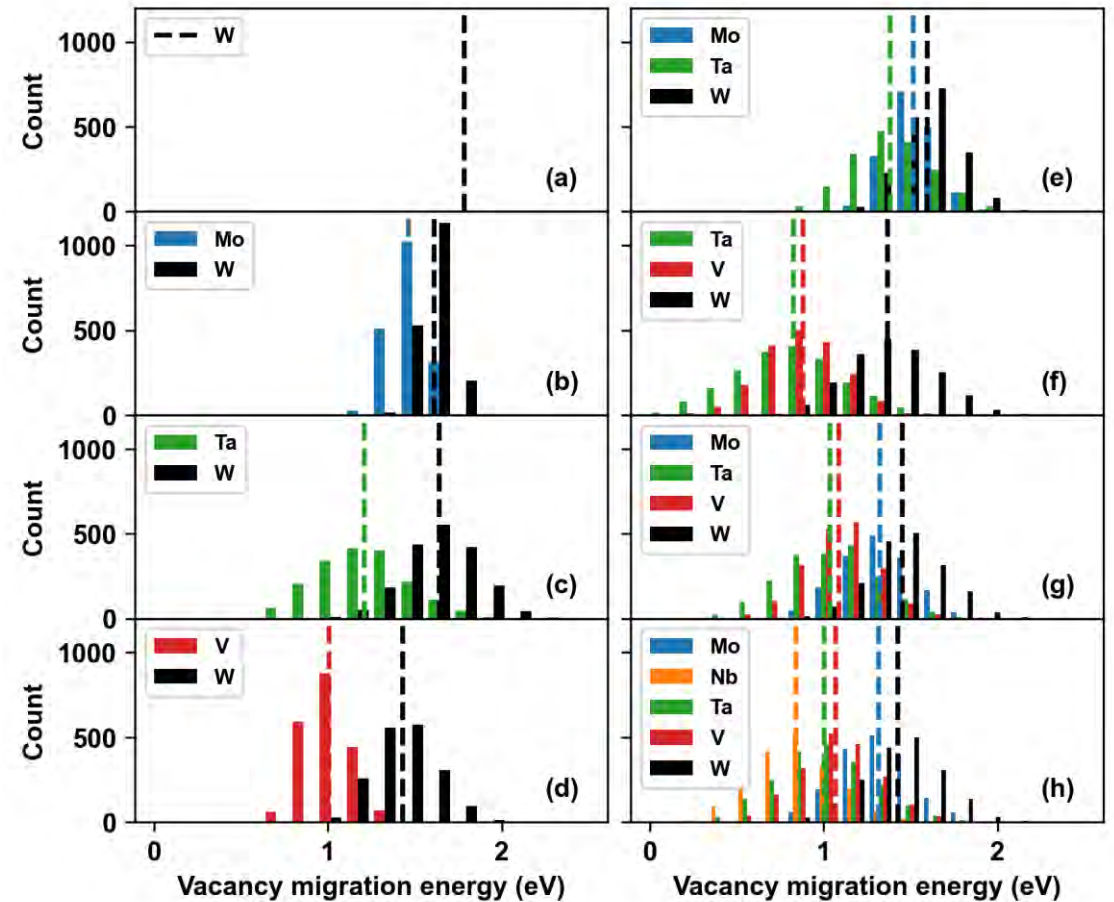


Fig.8: Distributions of vacancy migration energies in different randomly ordered surroundings in the considered materials as calculated with the nudged elastic band method (NEB). The distributions are the migration energy for each moving element and the dashed lines are the average values.<sup>16</sup>



# Segregation

	W <sub>Mo</sub>	W <sub>Ta</sub>	W <sub>TaMo</sub>	W <sub>V</sub>	W <sub>TaV</sub>	W <sub>TaVMo</sub>	W <sub>TaVMoNb</sub>
<b>Mo in SIA</b>	66.9%	-	70.3%	-	-	5.6%	4.9%
<b>Mo around Vac</b>	45.3%	-	31.5%	-	-	23.3%	17.8%
<b>Nb in SIA</b>	-	-	-	-	-	-	1.1%
<b>Nb around Vac</b>	-	-	-	-	-	-	28.4%
<b>Ta in SIA</b>	-	31.6%	11.1%	-	0.5%	0.2%	0.3%
<b>Ta around Vac</b>	-	57.4%	40.6%	-	45.3%	34.7%	24.6%
<b>V in SIA</b>	-	-	-	98.4%	98.0%	92.9%	92.2%
<b>V around Vac</b>	-	-	-	49.8%	29.6%	21.7%	16.3%
<b>W in SIA</b>	33.1%	68.4%	18.5%	1.6%	1.5%	1.3%	1.5%
<b>W around Vac</b>	54.7%	42.6%	27.9%	50.2%	25.1%	20.3%	12.9%

Tab.3: Atomic concentration in interstitial clusters and around vacancy clusters at a dose of 0.3 dpa.



# Annealing

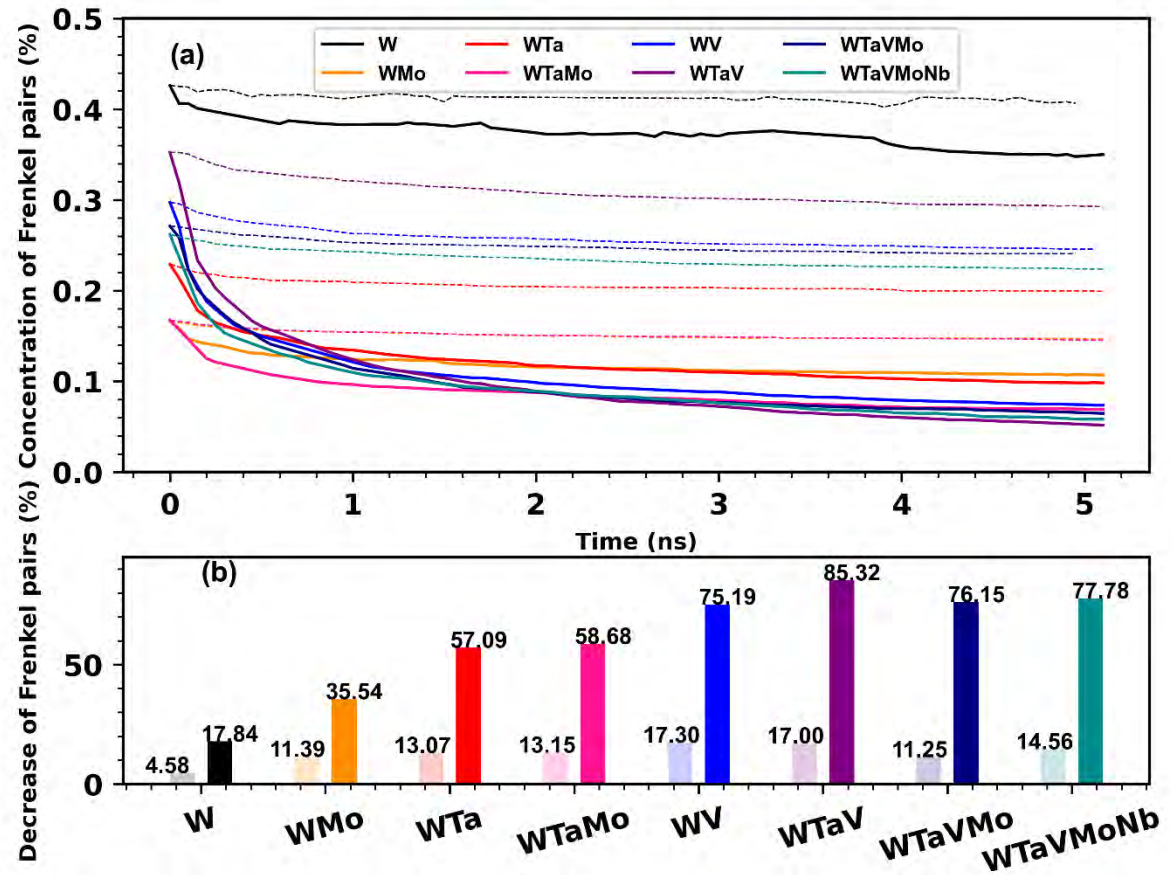


Fig.9: (a) The concentration of FPs during the annealing simulations at 0.3 dpa. Dashed lines correspond to annealing at 1000 K and solid lines correspond to annealing at 2000 K. (b) The decrease of FPs after annealing. Transparent bars correspond to annealing at 1000 K and solid bars correspond to annealing at 2000 K.



# Defect structures after annealing

- Mo
- Nb
- Ta
- V
- W
- Vac

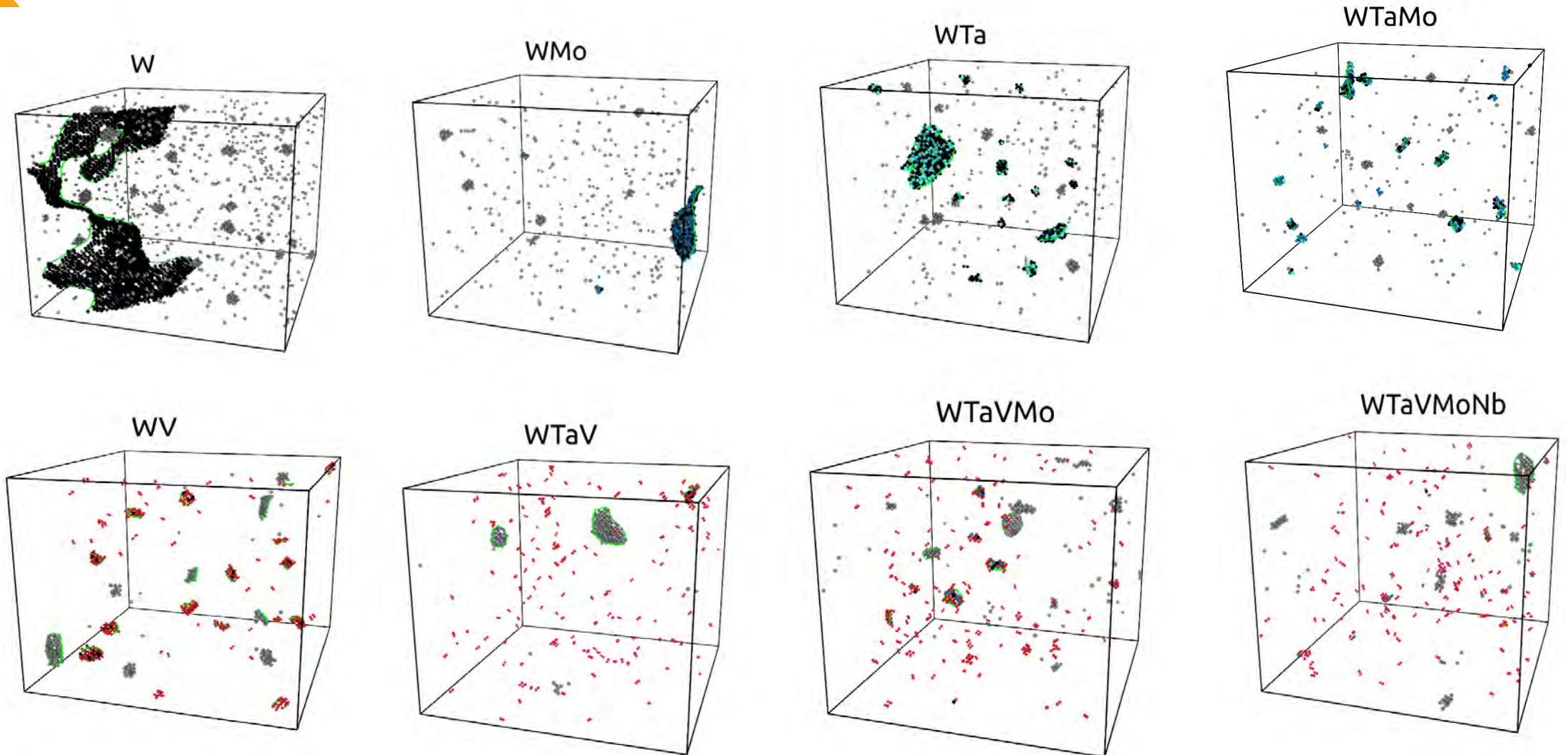


Fig.10: Defect snapshots for considered materials after 5 ns annealing at 2000 K. The atoms with different colours represent the different elements. The grey clusters represent the vacancy clusters. The green loops represent the  $\frac{1}{2}\langle 111 \rangle$  dislocation loops.



# Ongoing work

W

WMo

WTa

WV

WTaMo

WTaV

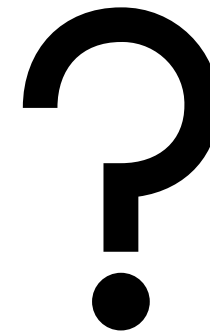
WTaVMo

WTaVMoNb

+ He



HerHEA





# Summary

## The presence of V:

- decreases the average threshold displacement energy
- balances the mobility of vacancies and interstitials
- causes efficient vacancy clustering directly in collision cascades
- promotes formation of vacancy loops due to increased binding energy relative to voids
- leads to formation of immobile V-rich interstitial clusters that remain small



EUROfusion



**Finnfusion Annual Seminar  
2024**



***Thank you for your attention!***